



HAL
open science

13th ERCOFTAC workshop on refined turbulence modelling, 25-26 th September, 2008, Graz University of Technology, Austria

H. Steiner, S. Jakirlic, G. Kadavelil, Remi Manceau, S. Saric, G. Brenn

► To cite this version:

H. Steiner, S. Jakirlic, G. Kadavelil, Remi Manceau, S. Saric, et al.. 13th ERCOFTAC workshop on refined turbulence modelling, 25-26 th September, 2008, Graz University of Technology, Austria. ERCOFTAC Bulletin, 2009, 79, pp.22-27. hal-00460705

HAL Id: hal-00460705

<https://hal.science/hal-00460705v1>

Submitted on 5 Nov 2020

HAL is a multi-disciplinary open access archive for the deposit and dissemination of scientific research documents, whether they are published or not. The documents may come from teaching and research institutions in France or abroad, or from public or private research centers.

L'archive ouverte pluridisciplinaire **HAL**, est destinée au dépôt et à la diffusion de documents scientifiques de niveau recherche, publiés ou non, émanant des établissements d'enseignement et de recherche français ou étrangers, des laboratoires publics ou privés.



Distributed under a Creative Commons Attribution - NonCommercial - NoDerivatives 4.0 International License

13th ERCOFTAC WORKSHOP ON REFINED TURBULENCE MODELLING

25-26th September, 2008, Graz University of Technology, Austria.

H. Steiner¹, S. Jakirlic², G. Kadavelil², R. Manceau³, S. Saric² and G. Brenn¹

¹ Institute of Fluid Mechanics and Heat Transfer Graz University of Technology, Austria.

² Institute of Fluid Mechanics and Aerodynamics Darmstadt University of Technology, Germany.

³ Laboratoire d'Etudes Aérodynamiques (LEA), Université de Poitiers, France.

Abstract

A report is given of the 13th ERCOFTAC SIG 15 Work-shop on Refined Turbulence Modelling, which was held at Graz University of Technology on 25th and 26th September, 2008.

1 Introduction

The role of the ERCOFTAC SIG15 (Special Interest Group for Turbulence Modelling) series of workshops on refined turbulence modelling is closely connected to intensive verification and systematic validation of CFD (Computational Fluid Dynamics) technology for solving problems of both fundamental importance and industrial relevance. Focus is on the credibility and reliability of both the numerical methods and mathematical models simulating turbulence. In such a way a large database of simulation results, along with detailed comparison with the reliable reference data (experimental, DNS and highly-resolved LES databases), has been assembled. The SIG15 workshops promote the discussion and conclusions about predictive performance of a variety of statistical turbulence models, SGS models in the LES-framework, as well as hybrid LES/RANS models in a broad range of well documented flow configurations among the scientists, researchers, users and developers from industry and from the academic field.

The 13th ERCOFTAC Workshop, hosted by the Institute of Fluid Mechanics and Heat Transfer at Graz University of Technology, Austria, was held on 25th and 26th September, 2008. The previous twelve workshops were organized in Lyon (1991), Manchester (1993), Lisbon (1994), Karlsruhe (1995), Chatou (1996), Delft (1997), Manchester (1998), Helsinki (1999), Darmstadt (2001), Poitiers (2002), Gothenburg (2005) and Berlin (2006). Unlike some previous workshops, where up to four complex 3-dimensional, unsteady flow geometries were treated (see for instance Thiele and Jakirlic, 2007), whose computation required several months or even years of intensive work (which could be provided only in the framework of a funded project), only two geometrically simpler benchmarks, but featured by complex flow and turbulence phenomena (3-D unsteady separation and reattachment, swirling effects, etc.) being of great scientific and engineering relevance were chosen as test cases for this workshop:

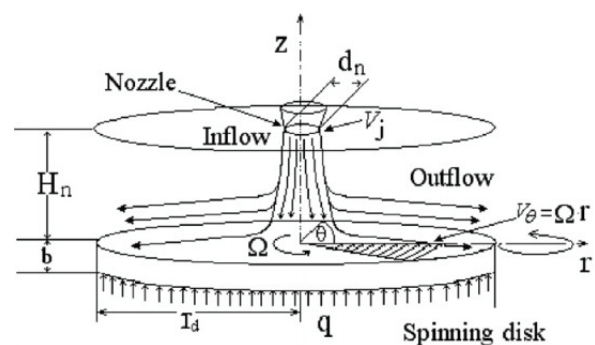


Figure 1: **SIG15 Case 13.1:** Round jet impinging perpendicularly onto a rotating, heated disc (Exp.: Popiel and Boguslawski, 1986; Minagawa and Obi, 2004). Schematic of the flow configuration considered showing the coordinate system used (adopted from Lallave et al., 2007).

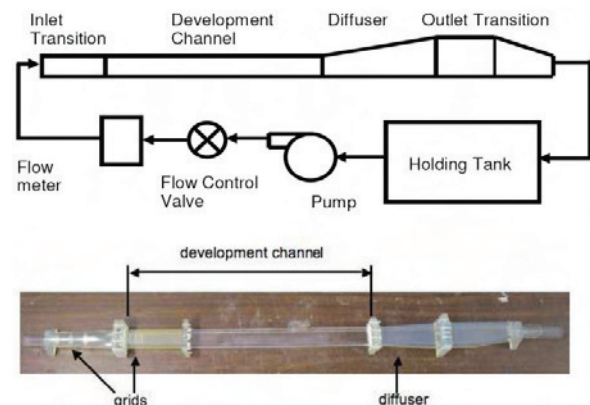


Figure 2: **SIG15 Case 13.2:** Separated flow in a 3-D diffuser. Experimental flow system schematic (Cherry et al., 2008, 2009).

Both cases have been selected for the first time. Relevant computational studies were performed by Benim et al. (2007) and Cherry et al. (2006). The second case represents a very recent experimental work.

In addition to the test case sessions, an oral session was organized accommodating up to ten lectures all dealing with hybrid RANS/LES computational methods with emphasis on their theoretical foundation and predictive capabilities in different applications. The oral

session was divided into a session accommodating the five survey lectures:

- *Addressing the near-wall problem in LES at high Reynolds numbers*, M. Leschziner (Imperial College London, UK)
- *PANS (Partially-Averaged Navier Stokes) method for turbulent flow simulations*, S. Girimaji, B. Basara (Texas A&M University, College Station, USA and AVL List GmbH, Graz, Austria)
- *Scale Adaptive Simulation (SAS): modelling concept and test cases*, F. Menter (ANSYS GmbH, Germany)
- *A new partially integrated transport modelling (PITM) method for continuous hybrid RANS/LES simulations*, B. Chaouat (ONERA, Palaiseau, France)
- *Detached-eddy simulation: overview, enhancements and example applications*, C. Mockett, (Technical University Berlin, Germany)

and a session containing the five flash presentations:

- *A hybrid LES-URANS approach based on Explicit Algebraic Reynolds Stress Models*, M. Breuer (LSTM, Univ. Erlangen-Nuremberg/Professorship for Fluid Mechanics, Helmut Schmidt University, Hamburg, Germany)
- *Examples of RANS/LES coupling using the Chimera method*, S. Benhamadouche (EDF R&D, Chatou, France)
- *Contribution of two- and three-point statistics to improved RANS and LES models*, C. Cambon (École Centrale de Lyon, France)
- *Consistency and invariance issues in developing a global hybrid RANS/LES method: temporally filtered PITM (T-PITM)*, A. Fadai-Ghotbi, R. Manceau, T. Gatski (LEA, Université de Poitiers, CNRS, France)
- *Large-Eddy Simulation of atomizing high-speed liquid jets*, D. Heidorn, H. Steiner, (Graz University of Technology, Austria)

The presentation files of all lectures and workshop proceedings can be downloaded from the workshop web site (<http://130.83.243.201/ercoftac-sig15/workshop2008.html> or www.ercoftac.org).

2 Participation

The 13th Workshop was attended by 50 participants from Europe, U.S.A. and Japan (13 from Germany, 15 from Austria, 6 from France, 2 from the United Kingdom, 1 from Denmark, 2 from Sweden, 1 from the USA, 1 from Japan, 1 from Italy, 3 from Hungary, 2 from Croatia, 2 from Slovenia, 1 from Bosnia & Herzegovina), of which 10 from industry, 4 from research institutes and 36 from universities.

3 Short Summary of Results and Discussion

Flow description, instructions for calculations, detailed specification of the shape and dimensions of solution domains, as well as of the inlet data and boundary conditions for the two test cases considered, are given in the workshop proceedings. Here, only a short description of the test cases and a summary of some specific outcomes and the most important conclusions are given.

SIG 15 Case 13.1: Round jet impinging perpendicularly onto a rotating, heated disc

A turbulent jet at Reynolds number $Re_j = 14500$ impinging perpendicularly onto a rotating disc (Fig. 1) represents the workshop's first test case. Detailed velocity measurements in the turbulent boundary layer developing on a rotating disk were conducted by Minagawa and Obi (2004). The rotation of the disk onto which the jet is impinging is at the origin of a skewing of the wall jet created around the impingement point. Therefore, this case provides an excellent example of a two-dimensional (axisymmetric) flow subject to a complex, six-component strain, pertinent to the investigation of the effects present in complex 3D-flows.

The effect of rotation is primarily manifested through the centrifugal acceleration and the mean flow skewing. The intensification and thinning of the radial wall jet due to centrifugal acceleration strongly promotes turbulent fluctuations in the radial direction. The shear strain $\partial V_\theta / \partial z$ leads to the appearance of shear stresses (compared to the case without rotation) and the intensification of the normal stress in the circumferential direction. Other stress components are indirectly affected, mainly by the redistribution process.

The shape of the solution domain and applied boundary types are indicated in Fig. 3. The flow configuration can be considered as axi-symmetric and steady. Accordingly, 2D computations can be performed when applying the RANS method. The necessary variable profiles at the inflow boundary into the solution domain (within the pipe) are to be obtained by precursor computations of the fully-developed pipe flow with corresponding turbulence models. As shown in Fig. 3, the upper boundary (inflow and pressure/Neuman boundary conditions) are located well above ($5D$) the pipe outlet, such that a significant portion of the pipe is included in the computational domain. At the disk wall, the rotational velocity (and the temperature) is prescribed, as given in the experiments.

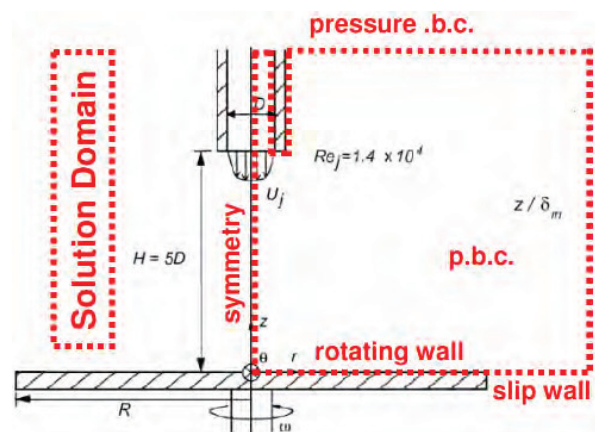


Figure 3: Solution domain and boundary conditions for the SIG15 Case 13.1.

Four different cases with respect to four rotational intensities from $\omega D / U_j = 0$ (non-rotating case) to $\omega D / U_j = 0.45$ were computed. Additionally to the above described computations of the mean flow and turbulence quantities, the heat transfer from the heated disc in accordance to the experiment of Popiel and Boguslawski was considered. The jet Reynolds number being closest to the Minagawa/Obi experiment is $Re_j = 46000$.

The computational groups contributing to this case and the turbulence models used are listed in Table 2. Accordingly, several versions of eddy viscosity models employing different scale-supplying variables (total viscous dissipation rate ε and a specific dissipation rate $\omega \sim \varepsilon/k$) and wall boundary treatment (wall functions and exact boundary conditions) were used. In addition, both Eddy-Viscosity models ($v^2 - f$ and $\zeta - f$, with $\zeta = v^2/k$; the latter model version is due to Hanjalic et al., 2004) and Second-Moment Closure models relying on Durbin's elliptic relaxation theory were applied.

Affiliation Author	Model	Acronym
International University of Sarajevo M. Hadziabdić	$\zeta - f$	IUS/ $\zeta - f$
Electricité de France S. Benhamadouche & P. Fourment	$k - \varepsilon$	EDF/ $k - \varepsilon$
	$k - \varepsilon$ linear production	EDF/ $k - \varepsilon$ -LP
	$k - \omega$ -SST	EDF/ $k - \omega$ -SST
	SSG RSM	EDF/SSG
Merkle & Partner GbR Carsten Horn	$k - \varepsilon$	MP/ $k - \varepsilon$
	$k - \omega$ -SST	MP/ $k - \omega$ -SST
University of Poitiers R. Perrin & R. Manceau	$k - \omega$ -SST	UP/ $k - \omega$ -SST
	Elliptic-Blending RSM	UP/EB-RSM

Table 1: SIG15 Case 13.1 - Contributors and models.

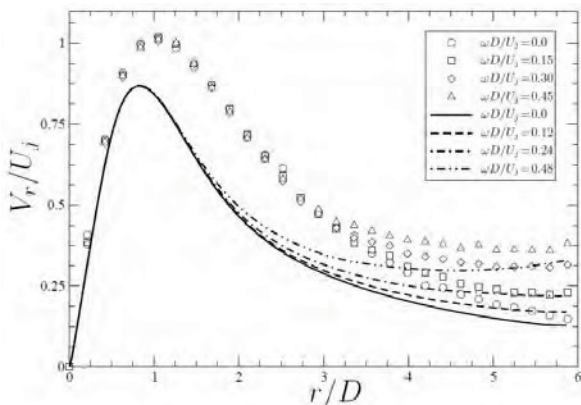


Figure 4: Development of the mean (V_r) radial velocity within the wall jet at $Z/D = 0.032$.

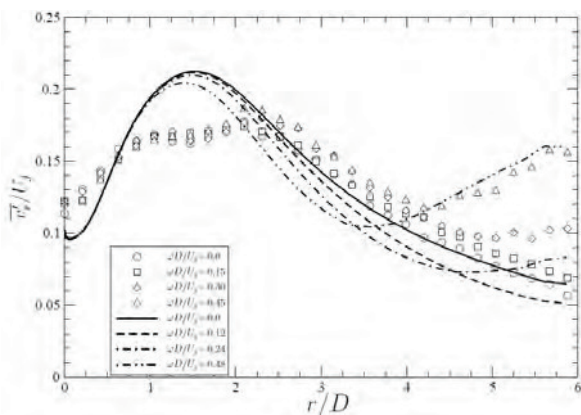


Figure 5: Development of the root-mean-square (v'_r) radial velocities within the wall jet at $Z/D = 0.032$.

Fig. 4 illustrates the evolution of the mean radial velocity in terms of the rotational intensity. The influence of the centrifugal acceleration becomes especially visible in the wall jet for larger distances from the axis of rotation ($r/D > 2.5$). The resulting acceleration of the mean flow in the radial direction (and thinning of the wall jet thickness, which can be seen on profiles along the vertical direction; not shown here) is reproduced independently of the turbulence model applied (the results shown here are obtained by the EB RSM model) because of the direct influence of rotation on the velocity field through the term in the momentum equation representing the centrifugal force.

A consequence of the modification of the velocity field is manifested through the intensification of the shear rate $\partial V_r/\partial z$, and in turn, of the corresponding turbulence production terms. The strong increase of the radial fluctuation v'_r due to intensification of its leading production term can be seen in Fig. 5. Such an effect is captured by all the models, even eddy-viscosity models, which include the direct influence of the shear stress. However, eddy-viscosity models give a much too early ($r/D = 2$ rather than $r/D = 4$) increase of v'_r , which can be traced to the fact that the production is assumed quadratic in the shear stress rather than linear.

The effect of the modification of the production in the Reynolds stress transport equations due to involvement of the secondary shearing $\partial V_\theta/\partial z$ (compared to the non-rotating case), which also modifies the turbulence anisotropy and the redistribution among the components, is documented in Fig 6. Expectedly, such an effect can only be captured by a Reynolds stress model.

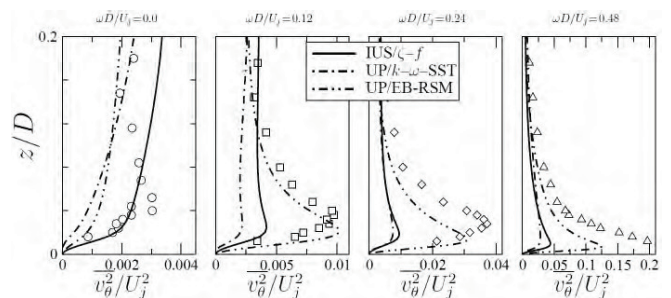


Figure 6: Profiles of $\overline{v_\theta^2}$ at $r/D = 5.8$ in terms of increasing rotation rates.

SIG 15 Case 13.2: Separated flow in a 3-D diffuser

An incompressible fully-developed duct flow expanding into a diffuser whose upper and one side walls are appropriately deflected, for which the experimentally obtained reference database was provided by Cherry et al. (2008, 2009), represented the workshop's second test case, Fig. 2. This flow configuration is characterized by a complex three-dimensional flow separation being the consequence of an adverse pressure gradient evoked by the duct expansion. It should be noted that two three-dimensional diffusers with the same fully-developed channel inlet, but slightly different expansion geometries, were experimentally investigated. Both diffuser flows exhibited three-dimensional boundary layer separation, but the size and shape of the separation bubble exhibited a high degree of geometric sensitivity to the dimensions of the diffuser. In the framework of the 13th workshop, only the first case (with the deflection angles of the upper and one

side wall being $\alpha = 11.3^\circ$ and $\alpha = 2.56^\circ$ respectively, Fig. 6) was computed. The second diffuser will be a test case of the forthcoming 14th workshop (which is to be held on September 18, 2009 at the Università di Roma ‘La Sapienza’, Italy: www.ercofac.org).

Experiments were performed to determine the mean velocity field. The streamwise Reynolds stress components have also been measured in the entire flow domain. In addition, the pressure coefficient distribution along the lower diffuser wall was provided (Cherry et al., 2009). Readers interested in more details about the measurement technique are referred to both experimental references. The dimensions of Diffuser 1 and the coordinate system are shown in Fig. 6. The inlet flow corresponds to fully-developed turbulence, and the bulk inlet velocity is 1 m/sec in the x direction, resulting in the Reynolds number of 10000. The origin of the coordinates coincides with the intersection of the two non-expanding walls at the beginning of the diffuser’s expansion.

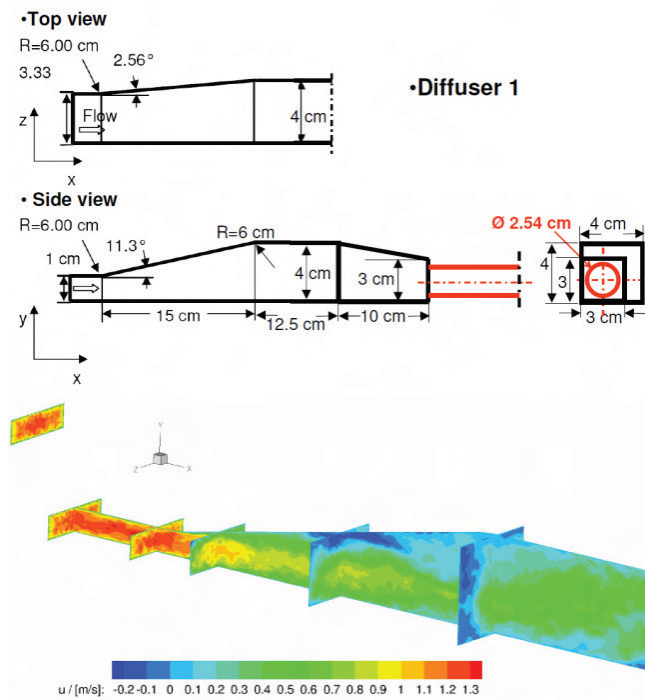


Figure 7: Geometry of the diffuser considered and the instantaneous velocity field obtained by LES (TU Darmstadt).

The following computational groups contributed to the comparative, cross-plot analysis:

- International University Sarajevo - IUS (Haddiadic)
- University Erlangen-Nuremberg (LSTM) / Professorship for Fluid Mechanics, Helmut Schmidt University, Hamburg (Breuer)
- Karlsruhe University (ITS and IFH Institutes; Schneider, von Terzi, Rodi)
- University of Manchester (Billard, Uribe, Laurence)
- Osaka Prefecture University (Suga)
- ANSYS GmbH Germany (Menter, Garbaruk, Smirnov)
- Università di Roma ‘La Sapienza’ (Borello, Hanzalic, Rispoli, Dalibra, Alfieri)

- Technische Universität Darmstadt (SLA and FNB Chairs; Kadavelil, Kornhaas, Saric, Sternel, Jakirlic, Schäfer)
- RWTH Aachen, E.ON Energy Research Center & Fa. Porsche (Brännström, Müller)

Unlike the first case, LES and LES-related methods (different seamless and zonal hybrid LES/RANS (HLR) models; DES - Detached Eddy Simulation), in addition to different RANS models, were massively applied here. The diversity of the models/methods applied can be seen from the following table.

Identifier	Organization	Method	grid
TUD LES	TU Darmstadt (FNB, SLA)	LES Dyn. Smag. Model (DSM)	4 Mio. cells
TUD DES		DES (S-A)	1.9 Mio. cells
TUD HLR		Hybrid LES-RANS SM+low-Re $k-\epsilon$ LS (1974)	1.9 Mio. cells
LSTM LES	University of Erlangen	LES Smag. Model (SM)	16 Mio. cells
LSTM HLR		Hybrid LES-URANS based on EARSM	2.8 Mio. cells
ITS LES	University of Karlsruhe	LES Smag. (SM) with wall functions	1.6 Mio. cells
ITS $k-\omega$ Wilcox		$k-\omega$ Wilcox	1.6 Mio. cells
ITS SA		Spalart-Allmaras	1.6 Mio. cells
UoM SST	University of Manchester	SST	1.1 Mio. cells
UoM PHIFBV2F		$\phi - \bar{j}$ Elliptic relaxation EVM	1.1 Mio. cells
UoM PHIALV2F		$\phi - \alpha$ Elliptic relaxation EVM	1.1 Mio. cells
UniOs $k-\epsilon$ + AWF	Osaka University	RANS Std. $k-\epsilon$	0.2 Mio. cells
UniOs CLS + AWF		NL EVM (3rd order)	0.2 Mio. cells
UniOs TCL + AWF		Craft, Launder, Suga RSM	0.2 Mio. cells
UniRo ZF	University of Rome	$k-\epsilon-\zeta-f$ Elliptic relaxation EVM	3.5 Mio. cells
UniRo HLR		Hybrid LES- $k-\epsilon-\zeta-f$	3.5 Mio. cells
IUS $k-\epsilon-\zeta-f$	University of Sarajevo	$k-\epsilon-\zeta-f$ Elliptic relaxation EVM	1.25 Mio. cells
VSH SST	Voith Siemens Hydro	$k-\omega$ SST	
VSH $k-\epsilon$		STD. $k-\epsilon$	
VSH SSG		DRSM Speziale, Sarkar, Gatski	
ANSYS SST	ANSYS	$k-\omega$ SST	
ANSYS WJ		Wallin & Johansson EARSM	
ANSYS EARSM		ANSYS EARSM	
ANSYS BSL-RSM		ANSYS baseline diff. RSM	

Table 1: SIG15 Case 13.2 - Contributors & methods.

The analysis of the results obtained has been conducted with respect to the size and shape of the flow separation pattern and associated mean flow and turbulence features. A selection of the computational results along with the experimental data is displayed in Figs. 7-9. Fig. 7 displaying the instantaneous velocity field obtained by LES provides a first impression of the flow topology. Figs. 8 show the contour plots of the axial velocity component in two selected streamwise cross-sectional areas, indicating the evolution of the flow separation pattern. Unlike the $k-\omega$ SST results, the results obtained by the LES and Hybrid LES/RANS methods agree reasonably well with respect to both the size and shape of the three-dimensional recirculation zone. The $k-\omega$ SST model resulted in a flow separating at the deflected side wall contrary to the experimental findings indicating the separation zone along the upper deflected

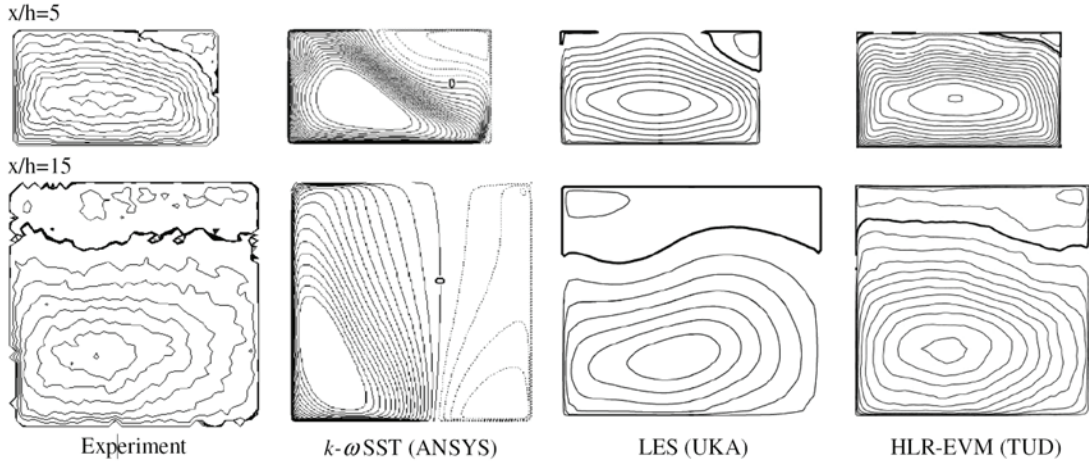


Figure 8: Iso-contours of the axial velocity field in the cross planes y - z at two selected streamwise locations within the diffuser section (the bold line denotes the zero-velocity line; $h = 1\text{cm}$)

wall. Similar results are obtained with all eddy-viscosity-based models applied. Keeping in mind the strong secondary motion across the inlet channel (characterized by jets directed towards the channel walls bisecting each corner and associated vortices at both sides of each jet) induced by the Reynolds stress anisotropy, which is, as generally known, beyond the reach of the eddy-viscosity model group, this outcome represents no surprise. The only RANS model which has correctly returned the flow topology was the ANSYS EARSM (Explicit Algebraic Reynolds Stress Model). Good agreement obtained with LES and hybrid methods is confirmed in Fig. 9 depicting the axial velocity and streamwise stress component profiles at 14 locations situated in all characteristic flow regions in a vertical plane corresponding to $z/B = 1/2$ ($B = 3.33\text{ cm}$). The results being closest to the experimental database, pertinent especially to the region bordering the recirculation zone, are those obtained by the University of Karlsruhe Group (Fig. 9 upper; denoted by UKA-LES) applying LES method on the grid with uniformly redistributed cells in conjunction with the wall functions for the near-wall treatment. It led to a finer grid resolution within the flow core compared to TUD-LES and HSU-LES (i.e. LSTM-LES). Both latter methods used fine near-wall resolution and integration up to the wall. Coarser grid resolution in the near-wall region and use of the wall-functions were justified by the fact that in this configuration the flow unsteadiness were introduced into the wall boundary layer from the core flow in accordance to the so-called ‘top-to-bottom’ process (communication with M. Leschziner).

4 Conclusions

Short summaries of the test cases description and the most important conclusions arising from the computationally obtained body of data are given in this report. In addition to the test case session, two oral sessions accommodating five survey lectures and five flash presentations were organized. This new format with two geometrically simpler benchmarks, but featured by complex flow and turbulence phenomena, led to a substantially improved attendance with 50 participants and computational results contributed by thirteen groups in total.

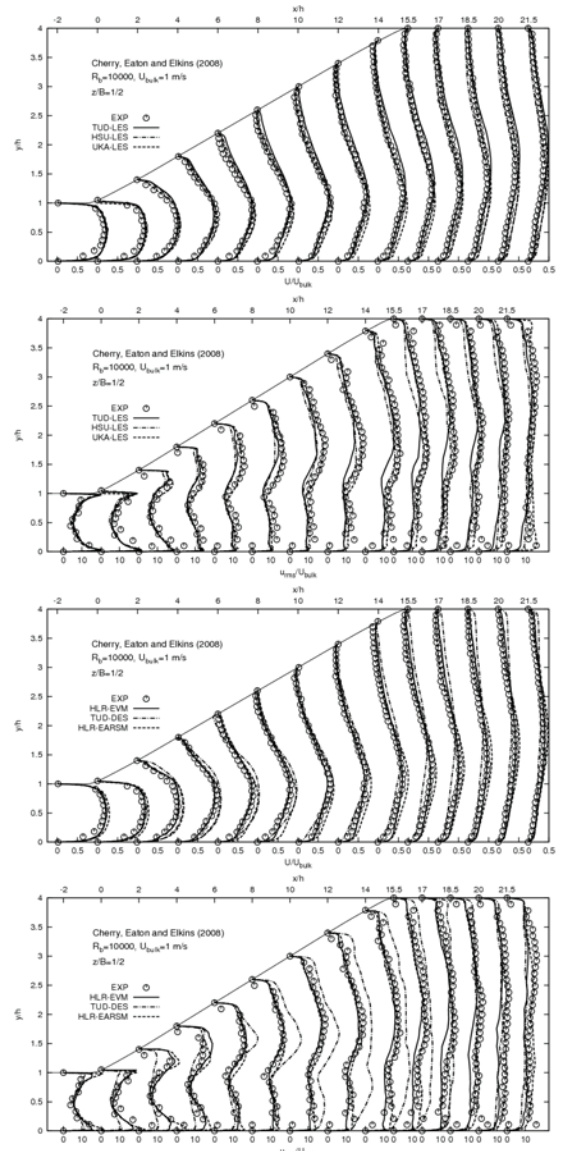


Figure 9: Evolution of the axial velocity and turbulent streamwise stress component profiles in the vertical plane x - y at the spanwise location $z/B = 1/2$: comparison between experiments and simulations.

Acknowledgements

We would like to thank the large number of people who were involved in the preparation and execution of this workshop. This applies especially to the SIG15 Steering Committee and the staff of the Institute of Fluid Mechanics and Heat Transfer at Graz University of Technology and the Chair of Fluid Mechanics and Aerodynamics in Darmstadt, who in one way or the other were all involved in the organization. We are thankful to the ERCOFTAC Administration/Development Office for the student grants. Our special thanks go to the reference data suppliers Erica Cherry (3D diffuser) and Shinnosuke Obi (impinging jet).

References

- [1] Benim, A.C., Ozkan, K., Cagan, M. and Gunes, D. (2007): *Computational investigation of turbulent jet impinging onto rotating disc*. *Int. J. Numerical Methods for Heat and Fluid Flow*, Vol. 17(3), pp. 284-301
- [2] Cherry, E. M., Iaccarino, G., Elkins, C.J. and Eaton, J.K. (2006): *Separated flow in a three-dimensional diffuser: preliminary validation*. Center for Turbulence Research, Stanford University, Annual Research Brief 2006, pp. 31-40
- [3] Cherry, E.M., Elkins, C.J. and Eaton, J.K. (2008): *Geometric sensitivity of three-dimensional separated flows*. *Int. J. of Heat and Fluid Flow*, Vol. 29, pp. 803-811
- [4] Cherry, E.M., Elkins, C.J. and Eaton, J.K. (2009): *Pressure measurements in a three-dimensional separated diffuser*. *Int. J. of Heat and Fluid Flow*, Vol. 30, pp. 1-2
- [5] Lallave, J.C., Rahman, M.M. and Kumar, A. (2007): *Numerical analysis of heat transfer on a rotating disk surface under confined liquid jet impingement*. *Int. J. Heat and Fluid Flow*, Vol. 28(4), pp. 720-734
- [6] Minagawa, Y. and Obi, S. (2004): *Development of turbulent impinging jet on a rotating disk*. *Int. J. Heat and Fluid Flow*, Vol. 25, pp. 759-766
- [7] Popiel, C. O. and Boguslawski, L. (1986): *Local Heat Transfer from a Rotating Disk in an Impinging Round Jet*. *ASME J. Heat Transfer*, Vol. 108, pp. 357
- [8] Thiele, F. and Jakirlic, S. (2007): *Report on 12th ERCOFTAC/IAHR/COST Workshop on Refined Turbulence Modelling*. October, 12-13, 2006, Technical University of Berlin, ERCOFTAC Bulletin, No. 75, pp. 5-10